Towards a Paleoearthquake Chronology for the New Madrid Seismic Zone:
Collaborative Research, M. Tuttle & Associates and Central Region Geologic Hazards Team, USGS

USGS Award No: 1434-HQ-97-GR-03082

Martitia P. Tuttle
M. Tuttle & Associates
HC 33 Box 48
Georgetown, ME 04548
Telephone: (207) 371-2796
FAX: (207) 371-2834
e-mail: mptuttle@erols.com

Project Element 1

Key Words: Paleoseismology, Paleoliquefaction, Age Dating

Abstract

A recent study in the New Madrid seismic zone demonstrates that large uncertainties, often involved but rarely expressed, in paleoliquefaction studies can be reduced by conducting detailed investigations at the most promising sites for dating liquefaction features. During the site investigations, care must be taken to collect samples that will provide close maximum and minimum dates for liquefaction features. It is advisable to use two-sigma calibrated dates, rather than one-sigma calibrated dates or radiocarbon ages, when estimating ages of liquefaction features. Well-constrained ages of individual liquefaction features should provide the basis for estimating the timing of paleoearthquakes and correlating features across a region. As uncertainty in ages of liquefaction features decreases, confidence in estimates of timing, source areas, and magnitudes of paleoearthquakes increases. The New Madrid study also shows that modern or historic earthquakes that induced liquefaction in the same region and whose locations and magnitudes are fairly well know can serve as calibration events for paleoearthquakes. Future efforts that could further improve the usefulness of liquefaction feature in paleoseismology include (1) the development of new techniques for dating liquefaction features directly, (2) case studies of modern earthquake that focus on the size and spatial distributions of liquefaction feature as well as geotechnical properties of liquefaction sites, and (3) more rigorous quantification of uncertainties associated with estimates of timing, source areas, and magnitudes of paleoearthquakes.

Introduction

Paleoseismology, or the study of fault rupture, ground shaking, and other earthquake effects as preserved in the geologic record, extends our knowledge of seismic activity into the prehistoric period, and thereby improves our understanding of the long-term behavior of fault zones or earthquake sources. Paleoseismology is proving especially useful in regions like eastern North America where strain rates are relatively low and recurrence intervals of large earthquakes are usually longer than the historical record. In eastern North America, where surface traces of seismogenic faults are uncommon or difficult to identify, most paleoseismology studies employ liquefaction features to learn about earthquakes that predate European settlement. Other features resulting from ground shaking also can be used (e.g., landslides, subaqueous slumps, and siltation layers in lacustrine deposits) but these involve greater uncertainties regarding their triggering mechanisms. Notable paleoliquefaction studies include those conducted in the meizoseismal areas of the 1727, body-wave magnitude (m_b) 5.6, Newbury, Massachusetts, earthquake (Tuttle and Seeber, 1991), 1811-1812, moment magnitude (**M**) 7.8 to 8.1, New Madrid, Missouri, earthquakes (e.g., Saucier, 1991; Li et al., 1998; Tuttle et al., 1996, 1999; Tuttle, 1999), 1886, **M** 7.5, Charleston, South Carolina, earthquake (e.g., Obermeier et al., 1985; Talwani and Cox, 1985; Amick et al., 1990), and 1988, **M** 5.9, Saguenay, Quebec, earthquake (Tuttle et al., 1992) as well as in the lower Wabash River valley of Indiana and Illinois (e.g., Munson et al., 1997; Obermeier et al., 1993). Drawing upon recent experience in the New Madrid seismic zone of the central United States, where the very large to great earthquakes of 1811-1812 produced world-class liquefaction features, this paper reviews the process of earthquake-induced liquefaction, the types of sedimentary deformation structures that result from liquefaction, and the methods used to estimate timing, source areas, and magnitudes of paleoearthquakes from liquefaction features.

Earthquake-Induced Liquefaction

A large body of literature discusses the triggering mechanisms and processes of liquefaction and fluidization as well as the sedimentary structures that form as a result of these processes. Important papers include Youd (1973), Lowe (1975), Seed (1979), Allen (1982), and Owen (1987). Earthquake-induced liquefaction is understood to be a process by which saturated, granular sediment temporarily loses its strength due to earthquake ground shaking (Seed and Idriss, 1982). As seismic waves generated by fault rupture propagate towards the ground surface, cyclic shear waves in particular distort the structure of near-surface sediment through which they pass. Densely packed soils will tend to dilate and not experience cyclic mobility. However, relatively cohesionless sediment that is water-saturated and loosely packed will tend to compact, leading to an increase in pore-water pressure. If pore-water pressure increases to the point that it equals overburden pressure, the sediment liquefies and behaves as a viscous liquid (Seed and Idriss, 1982). The resulting slurry of water and sediment will tend to flow towards the ground surface. The slurry may flow along pre-existing cracks and zones of weakness (Audemard and de Santis, 1991), along cracks that form during the passage of the seismic waves (Youd, 1984), along pathways that develop due to piping or hydraulic fracturing, and along tension fractures that form as a result of lateral spreading. Sedimentary structures that form as the result of earthquake-induced liquefaction, include sand blows, dikes, and sills. Sand blows are deposits that form on the ground surface due to venting of water and sand (Fig. 1). Sand blows bury pedogenic soil horizons and are connected to sand dikes. Sand dikes are sediment-filled cracks through which water and sand flowed. Sand sills usually take the form of lenses intruded below layers of low permeability and are structurally connected to sand dikes.

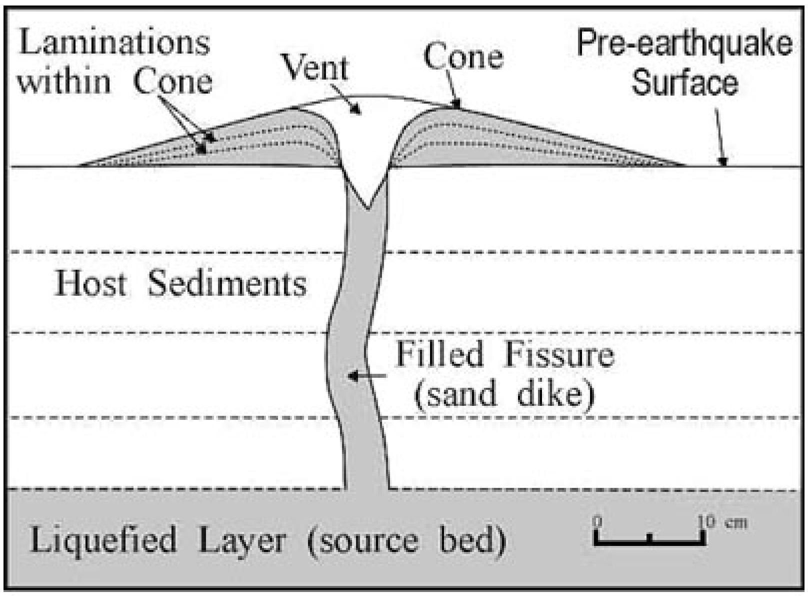

Figure 1. Schematic section showing sand blow and related liquefaction features with stratigraphic and structural relations (from Sims and Garvin, 1995).

<u>Recognizing Earthquake-Induced Liquefaction Features</u>

To be useful in paleoseismology studies, earthquake-induced liquefaction features must be distinguished from other types of soft-sediment deformational structures. Dewatering due to rapid sedimentation and compaction is one of the more common causes of syndepositional, non-seismic, liquefaction features (e.g., Lowe, 1975; Owen, 1987). Also, artesian pressure, piping, and diversion of runoff can lead to the formation of post-depositional sand boils that resemble liquefaction features (e.g., Holzer and Clark, 1993). However, earthquake-induced features can be differentiated from non-seismic structures through a combination of field evidence (e.g., distribution pattern, conduit morphology, sedimentary and stratigraphic characteristics of deposits, and material source) and laboratory x-ray radiography that reveals the internal flow of liquefied sediment (e.g., Sims, 1973; Li et al., 1996).

Descriptions of actual earthquake-induced liquefaction features, combined with laboratory modeling of liquefaction, provide the basis for identifying liquefaction features in the geologic record. Most large earthquakes around the world have generated liquefaction features; however, relatively few historical and modern liquefaction features have been studied in detail. Exceptions include features produced by the following earthquakes: 1811-1812 New Madrid, Missouri (Obermeier et al., 1990; Wesnousky and

Leffler, 1992; Tuttle, 1999), 1886 Charleston, South Carolina (Amick et al., 1990; Obermeier et al., 1990), 1971 San Fernando, California (Sims, 1973), 1988 Saguenay, Quebec (Tuttle et al., 1990, 1992), 1989 Falcon State, Venezuela (Audemard and de Santis, 1991), and 1989 Loma Prieta, California (Sims and Garvin, 1995). As synthesized by Obermeier (1996) and summarized below, criteria for identifying earthquake-induced liquefaction features include (1) sedimentary characteristics indicative of sudden, strong, upwardly-directed hydraulic force of short duration; (2) sedimentary characteristics consistent with case histories of earthquake-induced liquefaction; (3) occurrence of more than one type of liquefaction feature and of similar features at multiple locations; (4) occurrence in geomorphic settings where hydraulic conditions described in (1) would not develop under non-seismic conditions; and (5) age data to support both contemporaneous and episodic formation of features over a large area.

Estimating Timing of Earthquakes from Liquefaction Features

Using liquefaction features to estimate timing of paleoearthquakes is a multi-step process. It begins with the identification, detailed study, and dating of many individual liquefaction features across a region. This is followed by compilation and interpretion of age estimates of these liquefaction features, and possibly other paleoseismic deformation structures, in terms of timing of paleoearthquakes. Clustering of age estimates of liquefaction features is thought to reflect timing of paleoearthquakes. Confidence in timing of events increases as well-constrained age estimates are determined for more and more liquefaction features across a region.

Of the various types of liquefaction features, sand blows provide the best opportunity for dating paleoearthquakes. Organic material and cultural artifacts within a pedogenic soil horizon developed in or above a sand blow can provide minimum age estimates of the feature and thus help to limit the timing of the event. Organic material and cultural artifacts within a soil horizon buried by a sand blow can provide maximum, and in some circumstances approximate, age estimates of the event. In the case of sand dikes and sills, their maximum ages can be determined by dating the uppermost stratigraphic unit that they cross-cut or overlie. Given that sand dikes and sills may terminate several meters below the ground surface, the maximum ages of these liquefaction features may be hundreds to thousands of years older than the actual event. The minimum ages of sand dikes and sills can be determined by dating materials that clearly post-date the liquefaction features such as intruding roots and cultural pits. Also, deposits that overlie an unconformity that truncates these types of liquefaction features can provide a minimum age estimate. It is fairly uncommon, however, to find circumstances such as these that help to constrain minimum ages of sand dikes and sills. The current methodology of bracketing the age of liquefaction features by dating bounding horizons can lead to uncertainties in age estimates from a couple of hundred to thousands of years. It is important to constrain the ages of liquefaction features as narrowly as possible in order to differentiate closely timed (i.e., within several hundred years) events and to correlate features across a region. As discussed below, regional correlations often form the basis for estimating source areas and magnitudes of paleoearthquakes.

As with paleoseismology in general, radiocarbon analysis is the most common dating technique used in paleoliquefaction studies. Also, artifact analysis has been employed in regions where ceramic and projectile point chronologies are well established. In addition, soil development within liquefaction features and horizons bounding such features can help to estimate the age of liquefaction features. In those instances where tree growth is affected by liquefaction, dendrochronology holds promise for precise dating of paleoearthquakes. Before dendrochronology can be employed, however, regional chronologies for affected tree species must be developed. Similarly, palynology may be a useful for dating liquefaction features, if a regional pollen chronology is established.

In paleoliquefaction studies, it is fairly common to see radiocarbon ages, rather than calibrated dates, used to estimate the ages of liquefaction features. Since ^{14}C in the atmosphere has fluctuated through time due to variations in cosmic radiation, and recently to burning of fossil fuels and testing of nuclear devices, radiocarbon ages do not reflect the true ages of the analyzed samples (Stuiver et al., 1993). Radiocarbon ages can be easily converted to calibrated dates, which do reflect true ages, using well-established dendrocalibration curves. The few paleoliquefaction studies that do employ calibrated dates often use one-sigma, rather than two-sigma, results. In addition, some studies employ intercept dates of the dendrocalibration curve. It is advisable, however, to use the minimum and maximum dates of the two-sigma range to more accurately reflect uncertainties in radiocarbon dating. In most paleoliquefaction studies, radiocarbon results for many, possibly unrelated, features across a region (a minimum date here, a maximum date there) are lumped together and then interpreted in terms of timing of paleoearthquakes. Not only does this practice lead to large uncertainties regarding the timing of events, rarely acknowleded in these studies, but also to erroneous spatial correlations of liquefaction features. It is better to estimate ages of individual features where close minimum and maximum dates are available and then use the few features whose ages are well-constrained to interpret timing of paleoearthquakes.

Estimating Earthquake Source Area from Liquefaction Features

It is usually assumed that the size and spatial distributions of liquefaction features reflect the location of the source region of a paleoearthquake. More specifically, the regional distribution of similar-age features is thought to represent the meizoseismal area (where strong ground shaking would be felt) and the largest liquefaction features the epicentral area of a paleoearthquake. This is a first approximation and several recent earthquakes demonstrate that, in general, feature size attenuates with epicentral distance. However, it has also been observed that the distribution of liquefaction features can be irregular and not necessarily centered around or even within the meizoseismal area (e.g., 1988 Saguenay, Quebec, 1989 Loma Prieta, California, and 1994 Northridge, California). Factors that can influence the distribution of liquefaction features include earthquake characteristics, such as directivity and focusing of seismic waves, and site conditions, such as liquefaction susceptibility of sediments, local ground motion amplification, and topography. Some of these factors will not be known for paleoearthquakes. Although characterization of site conditions and modern and historic seismicity can contribute to more realistic interpretations, there will always be uncertainties in estimating earthquake source areas from liquefaction features. Case studies of liquefaction induced by modern and future earthquakes could help to further characterize the size and spatial distributions of liquefaction features. Such studies should include detailed descriptions of liquefaction features and evaluations of subsurface conditions at many sites over broad regions.

Estimating Earthquake Magnitude from Liquefaction Features

Several approaches have been used to estimate magnitudes of paleoearthquakes from liquefaction features. These approaches include (1) the relation between earthquake magnitude and maximum distance to liquefaction, (2) the relation between the liquefaction severity index and distance of liquefaction from the seismic energy source, (3) the simplified procedure for evaluating liquefaction potential and a modification of the procedure known as the seismic energy approach, (4) the relation between peak ground acceleration and thickness of liquefied sand and overlying deposits penetrated by sand dikes, and (5) the comparison of paleoliquefaction features with features resulting from modern or historic earthquakes in the same region. The first four approaches were originally developed for the purpose of assessing liquefaction or ground failure potential during future earthquakes. The ability of these approaches to accurately back-calculate magnitudes of earthquakes has yet to be demonstrated. The fifth approach is based on the geologic principle that modern geologic processes and their products provide a comparative basis for reconstructing past geologic events.

The relation between earthquake magnitude and maximum distance to surface evidence of liquefaction is founded on the assumptions that ground motion attenuates with distance from its seismic source and that at some epicentral distance ground motion for an earthquake of a given magnitude will be too weak to induce liquefaction. This relation was first developed from cases of liquefaction induced by earthquakes in Japan (e.g., Kuribayashi and Tatsuoka, 1975) and later modified to include data from earthquakes from other parts of the world. Ambraseys (1988) compiled an extensive liquefaction database, including earthquakes in areas of lower attenuation, differentiated between shallow and intermediate-depth earthquakes, and developed relations for both epicentral distance and distance from the seismic energy source or fault rupture. There are a few earthquakes that induced liquefaction at greater distance than most other earthquakes of comparable magnitude that fall outside the limiting bound of these relations. Depending on the seismotectonic setting of a study area, the more appropriate of Ambraseys' relations can be used to estimate the minimum magnitude of a paleoearthquake. Earthquake characteristics, such as frequency content, duration, and stress drop, that influence whether or not sediment liquefies are not known for paleoearthquakes. Therefore, uncertainties on the order of perhaps a quarter of a magnitude unit should be attached to magnitudes of paleoearthquakes estimated with Ambraseys' relations.

The liquefaction severity index (LSI) is a measure of ground failure displacement related to lateral spreading on gently sloping late Holocene fluvial deposits (Youd and Perkins, 1987). LSI represents the maximum observed severity of ground failure at a given locality, with displacements greater than 2.5 m receiving the limiting value of 100. Values of LSI have been determined for several earthquakes, ranging in magnitude from

M 5.2 to 9.2, in the western United States (U.S.) and plotted against horizontal distance from fault rupture. A relation has been developed for one modern and two historic earthquakes the eastern U.S. and Canada that shows liquefaction at greater distances in this region compared to similar-size earthquakes in the west. Liquefaction at greater distances is probably due to lower attenuation of ground motion in the relatively old and hard crystalline rocks of eastern North America. Although they have been employed only rarely in paleoliquefaction studies, LSI-distance relations allow for the use of liquefaction features, including sand blows, in the meizoseismal area and do not rely on distal liquefaction features, often sand dikes, that may be difficult to date with tight age constraints and attribute to one particular paleoearthquake.

The simplified procedure for evaluating liquefaction potential relies on geotechnical data at liquefaction and non-liquefaction sites to estimate peak ground acceleration (Seed et al., 1983, 1985). The application of the simplified procedure in paleoliquefaction studies involves an iterative process that uses accelerations generated by hypothetical earthquakes of various magnitudes and epicentral distances necessary to generate the observed distribution of liquefaction features. Uncertainties in attenuation relations, especially in regions of few instrumentally-recorded earthquakes, can have a significant affect on magnitude estimates derived in this manner. The seismic energy approach developed by Pond (1996) is very similar to the Seed et al. procedure except that it uses an estimate of seismic energy, rather than peak acceleration, to evaluate liquefaction at sites of interest.

The relations between peak ground acceleration and thickness of liquefied sand and overlying deposits penetrated by sand dikes is based on only a few earthquakes of M ~7.5 (Ishihara, 1985). More recently, Youd and Garris (1995) considered additional earthquakes covering a broader magnitude range and found that the relations do not apply in situations where lateral spreading is involved. In cases of paleoliquefaction, it can be difficult to assess whether or not lateral spreading played a role in the formation of sand dikes. The topography and geologic relations that may have influenced ground failure, as well as the geologic record of ground failure, may be considerably modified since the time of the liquefaction event. In addition, it can be difficult to know the absolute height of a sand dike, rather than its apparent height as exposed in a geologic section. Since sand dikes pinch out vertically as well as laterally, multiple trenches may be required to determine the absolute height of a dike. In cases where sand dikes are exposed in river or ditch cutbanks, the absolute height of dikes may never be known since large portions of them may have been removed during cutbank erosion. As mentioned above, it is often difficult to constrain the age of sand dikes. If recurrent liquefaction has occurred at a site and ages of the sand dikes can not be differentiated, not only may a liquefaction event be overlooked but also the wrong generation of sand dikes could be used to estimate acceleration. Given the many uncertainties in determining the age and absolute height of sand dikes, the relations developed by Ishihara may not be appropriate for back-calculating accelerations and magnitudes of paleoearthquakes, except in very unusual circumstances.

The comparison of paleoliquefaction features with modern or historic features for the purpose of estimating magnitudes of past earthquakes follows the geologic principle of actualism, also known as the doctrine of uniformitarianism. The principle of actualism was succinctly expressed by Sir Archibald Geikie as, "The present is the key to the past." In this application of the principle, the size and spatial distributions of liquefaction features induced by modern or historic earthquakes, whose locations and magnitudes are fairly well known, are used to interpret the size and spatial distribution of paleoliquefaction features attributed to a particular paleoearthquake (Tuttle, 1999). Since conditions affecting liquefaction susceptibility (e.g., density of liquefied layer, overburden, depth of water table) may have changed between events, there are uncertainties associated with magnitude estimates of paleoearthquakes using this approach as well.

Although not yet applied in paleoseismology, Arias intensity may be useful for estimating magnitudes of paleoearthquakes. Arias intensity is a measure of the total energy per unit weight that would be absorbed during earthquake shaking by undamped linear oscillators evenly distributed in frequency (Arias, 1970; Kayen and Mitchell, 1997). Arias intensity is calculated by integrating accelerograms recorded at given site. For some applications, however, it can be estimated from previous Arias intensity response at a site, Arias intensity predictor equations, or site response modeling (Kayen and Mitchell, 1997). Wilson (1993) developed a relation of Arias intensity to earthquake magnitude and source distance, which Kayen and Mitchell (1997) later modified specifically for alluvial, soft-soil, and rock sites. So far, Arias intensity predictor equations are based on ground motion records from the western U.S., primarily California. The application of Arias intensity in paleoliquefaction studies would require characterization of the soil column using field penetration tests. In addition, it would probably be necessary to calibrate Arias intensity predictor equations for regions where ground motion attenuation differs from that in the western U.S.

Paleoliquefaction Study in the New Madrid Seismic Zone

The New Madrid seismic zone (NMSZ) is the most seismically active region in the U.S. east of the Rocky Mountains (Fig. 2). Holocene sand blows are abundant in the New Madrid region and cover from 1 percent to more than 25 percent of the land surface over a 10,000 km^2 area (Saucier, 1977; Obermeier, 1989). In the past, these sand blows were attributed to an earthquake sequence that struck the region during the winter of 1811-1812. It is now clear that this large liquefaction field is composed of pre-1811 as well as historic sand blows. World-class liquefaction features offer an excellent opportunity to estimate the timing, location, and magnitude of large paleoearthquakes in the NMSZ. Several important lessons that advance the use of liquefaction features in paleoseismology have been learned from studying liquefaction in this region.

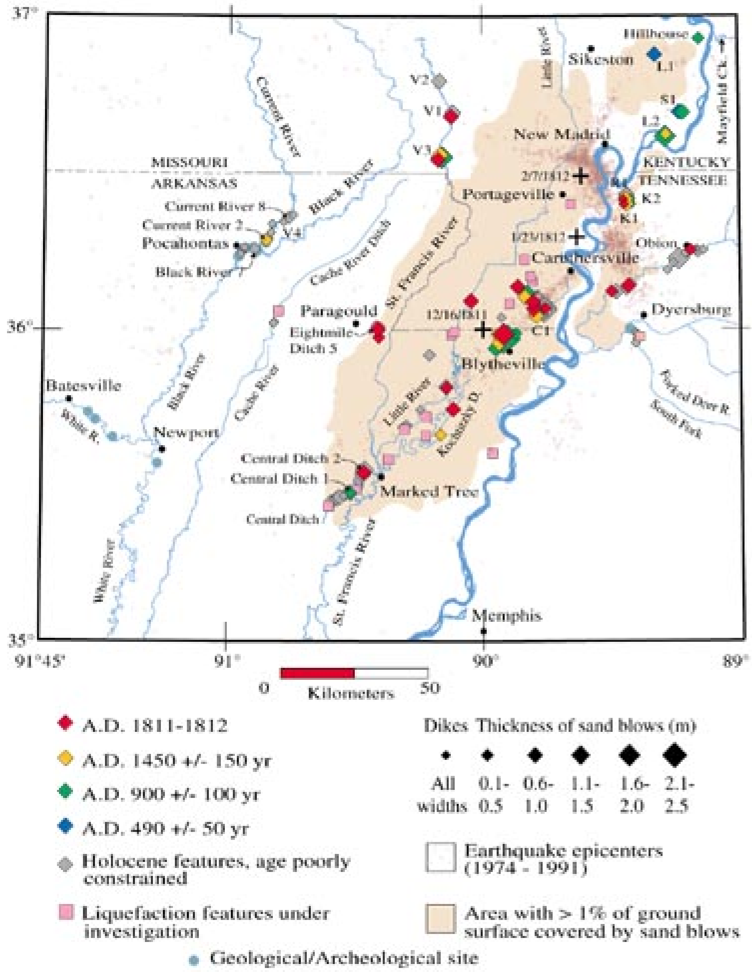

Figure 2. Map of New Madrid seismic zone showing estimated ages and sizes of liquefaction features. All sites in Tuttle (1999) except R1, Russ (1982); S1, Saucier (1991); Craven (1995); L1 and L2, Li et al. (1998); K1 and K2, Kelson et al. (1996); V1-4, Vaughn (1994). Area of surficial sand blow deposits (Obermeier, 1989).

<u>Geologic and Seismotectonic Setting</u>

Since 1974, seismic networks have recorded thousands of small to moderate earthquakes that define several seismicity trends or branches of the NMSZ in the northern part of the Mississippi embayment (Fig. 2). The Mississippi embayment is a broad southwest plunging syncline filled with Late Cretaceous and Paleogene marine sedimentary rocks and Pliocene and Quaternary fluvial sediments (Fig. 3; Murray, 1961; Buschbach and Schwalb, 1984). Late Quaternary sediments within the Mississippi embayment are 30 to 60 m thick and are predominantly Wisconsin valley train and Holocene meander belt deposits of the Mississippi, St. Francis, and White Rivers and their tributaries (Fig. 4; Saucier, 1994). The Mississippi embayment is underlain by Paleozoic sedimentary and basement rocks intruded by Late Paleozoic/Triassic mafic and Middle Cretaceous ultramafic and alkalic igneous rocks (Buschbach and Schwalb, 1984). A thickened basal crustal layer interpreted from gravity data as the Reelfoot rift corresponds with the area of greatest seismic activity (Braile et al., 1988). It is thought that New Madrid seismicity is due to reactivation of rift structures by contemporary, east-northeast (N80°E) oriented, regional compressive stress resulting from plate motions (Braile et al., 1988; Zoback and Zoback, 1989).

In the winter of 1811 and 1812, the NMSZ generated an earthquake sequence that included three very large to great earthquakes. The three largest earthquakes in this sequence are estimated to be of moment magnitude **M** 7.8 to 8.1 (Johnston, 1996) and were felt as far away as Hartford, Connecticut, Charleston, South Carolina, and New Orleans, Louisiana (Street and Nuttli, 1984). In the northern part of the Mississippi embayment, these earthquakes caused widespread liquefaction (Fig. 2; Fuller, 1912; Saucier, 1977; Obermeier, 1989) and severe ground failure (Tuttle and Barstow, 1996). Liquefaction was reported about 200 km northeast of the NMSZ in White County Illinois, 240 km to the north-northwest near St. Louis, Missouri, and 250 km to the south near the mouth of the Arkansas River (Johnston and Schweig, 1996). Although the exact magnitudes of the earthquakes are debatable, there is no doubt that a repeat of an 1811-1812 New Madrid sequence today would cause a great deal of damage in the central United States.

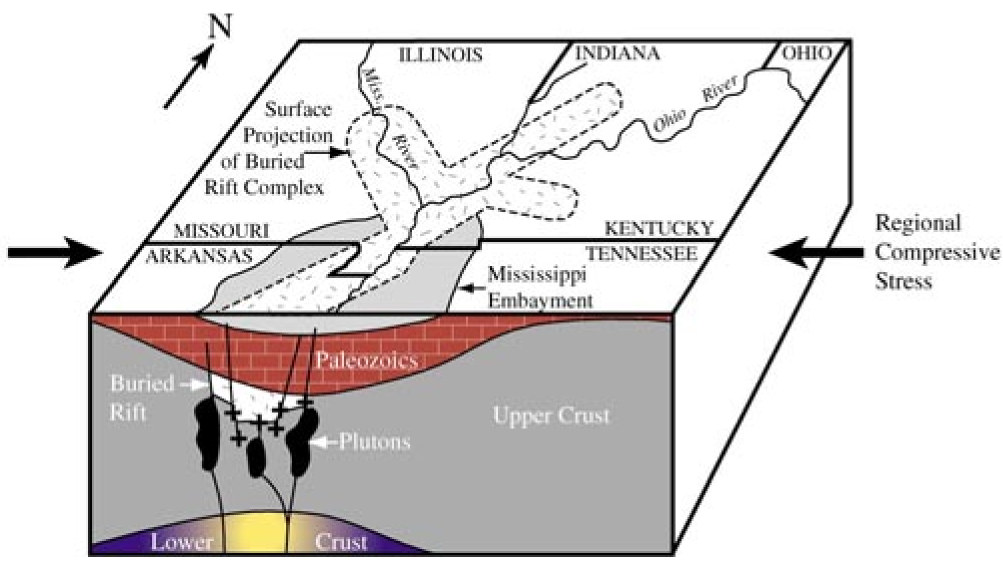

Figure 3. Tectonic model of New Madrid seismic zone (modified from Braile et al., 1984).
Seismicity in lower crust is thought to be related to reactivation of faults of Reelfoot rift system within current stress field.

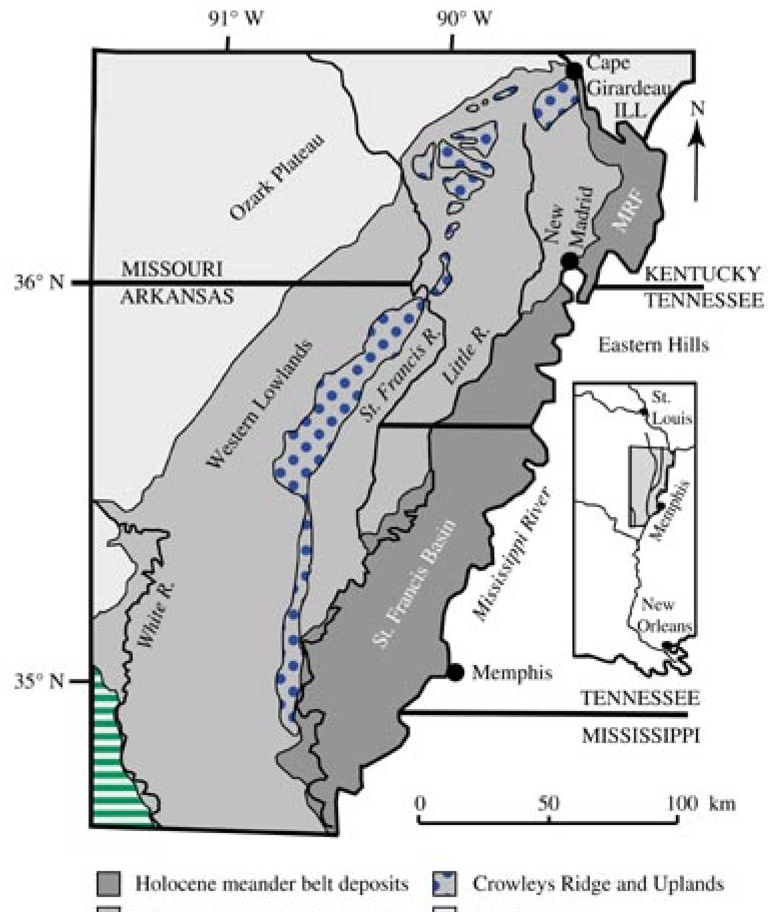

[redacted]

Figure 4. Generalized map of Mississippi River alluvial valley (modified from Saucier, 1994). MRF, Mississippi River floodway.

<u>Results of Paleoliquefaction Studies</u>

During reconnaissance in the NMSZ, liquefaction features have been found, described, and measured at more than one hundred and twenty sites (Fig. 2). Sand blows appear as light-colored sandy patches on the ground surface (Fig. 5). In plan view, sand blow deposits have circular, elliptical, and linear shapes and can range up to tens of meters in width and hundreds of meters in length. In cross-section, sand blows commonly take the form of large, constructional cones 1 to 2 m in thickness. Sand blow deposits are characterized by (1) fining upward sequences of coarse sand to silt that fine and thin away from sand dikes, (2) sedimentary structures that indicate fluid flow away from the sand dikes, (3) complex cross-cutting relations above dikes, (4) and rip-up clasts of underlying deposits and soil horizons that tend to be larger and more concentrated above sand dikes than at some distance (meters) from dikes (Fig. 6). Subsidence of the ground surface, due to removal of subsurface material during venting, is often associated with sand blows. Sand dikes crosscut deposits and soils horizons, may exhibit subvertically oriented bedding and complex cross-cutting relations, and often contain rip-up clasts of host deposits and soil horizons (Fig. 7). Observations made during reconnaissance indicate that paleoearthquakes, as well as the 1811-1812 earthquake sequence, induced liquefaction over a broad region. Liquefaction features that formed during the 1811-1812 and earlier earthquakes occur within and beyond the area of surficial sand blows mapped by Saucier (1977) and Obermeier (1989). The full extent of liquefaction resulting from paleoearthquakes generated by the NMSZ has not yet been defined.

As of June 1999, detailed investigations of liquefaction features had been conducted at twenty-five sites (Tuttle et al., 1996, 1999; Tuttle, 1999). In addition, Russ (1982), Saucier (1991), Vaughn (1994), Craven (1995), Wesnousky and Johnson (1996), and Li et al. (1998) carried out investigations at another twelve liquefaction sites. Taken together, these investigations provide well-constrained ages for a number of liquefaction features, and thus the timing of earthquakes that led to their formation (Fig. 8). In addition, the investigations reveal the size distribution of liquefaction features that helps to estimate the locations and magnitudes of paleoearthquakes (Fig. 9). See Tuttle (1999) for descriptions of liquefaction features documented during the reconnaissance and related site investigations.

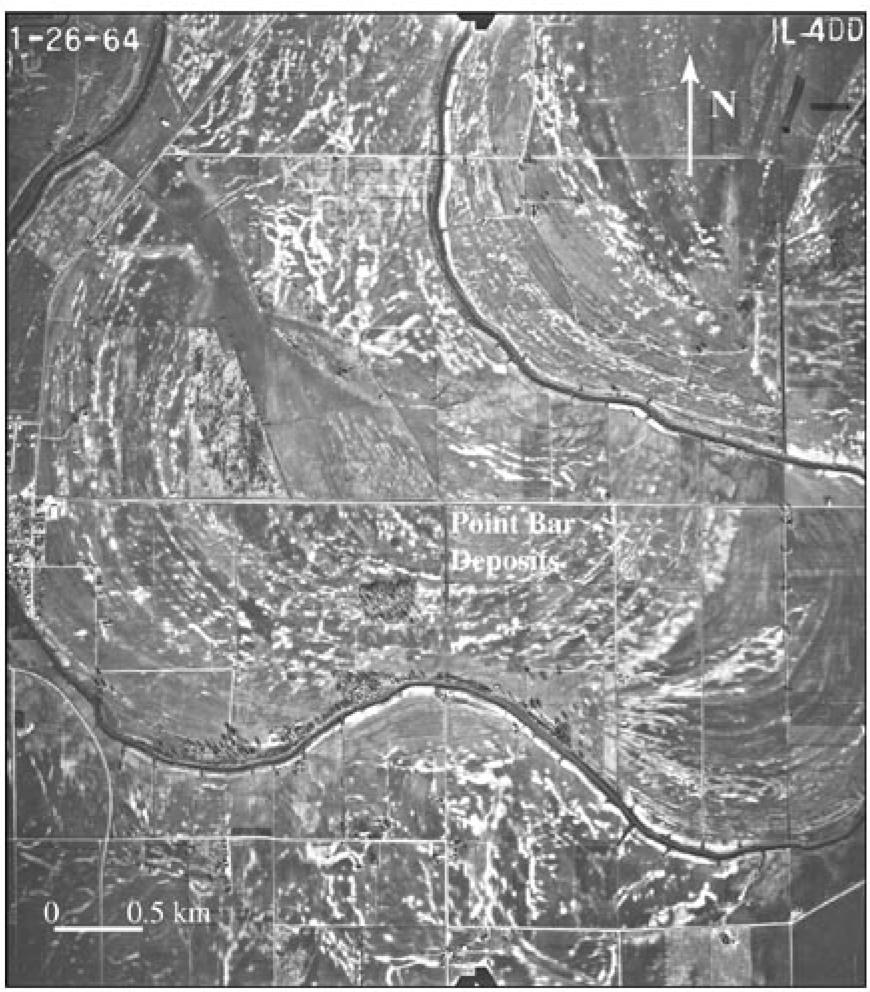

Figure 5. Aerial photograph showing light-colored sand blows near Pemiscot Bayou

(taken by U.S. Department of Agriculture on January 26, 1964). Notice sand blows follow scroll pattern of point bar deposits within meander bends, suggesting that these laterally accreted deposits have contacts that serve as preferred pathways for slurries of sand and water resulting from liquefaction (J. Tinsley, pers. comm., 2000).

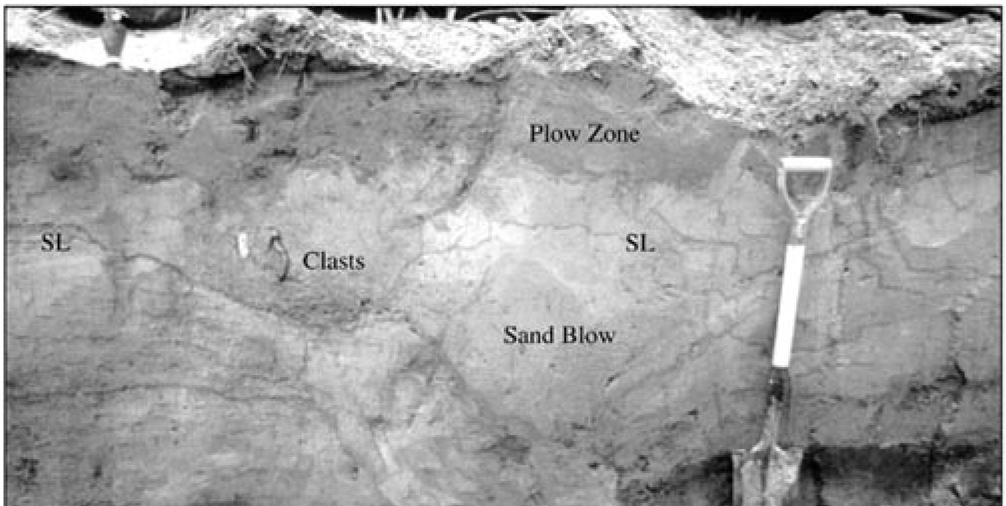

Figure 6. Photograph of sand blow and related feeder dike exposed in trench. Sand blow buries pedogenic soil that was at ground surface at time of event. Soil lamellae (SL) in sand blow suggest that it is prehistoric in age. For scale, shovel blade is 20 cm wide.

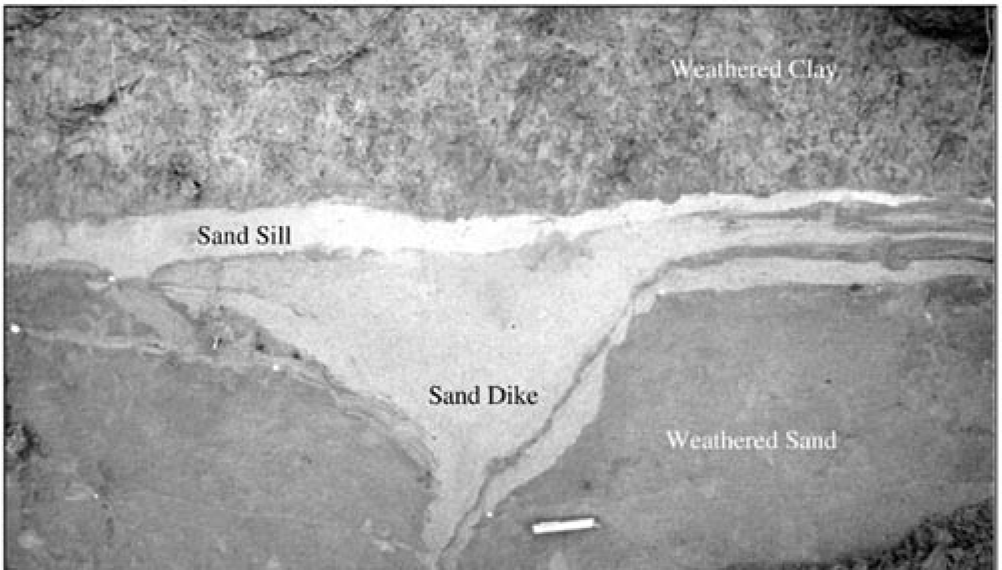

Figure 7. Photograph of sand dikes and sills exposed in ditch cutbank in the NMSZ. Sand dike intruded
through weathered sand and sand sills intruded along base of weathered clay deposit. Sills may have been
intruded during two different events. For scale, knife is 9 cm long.

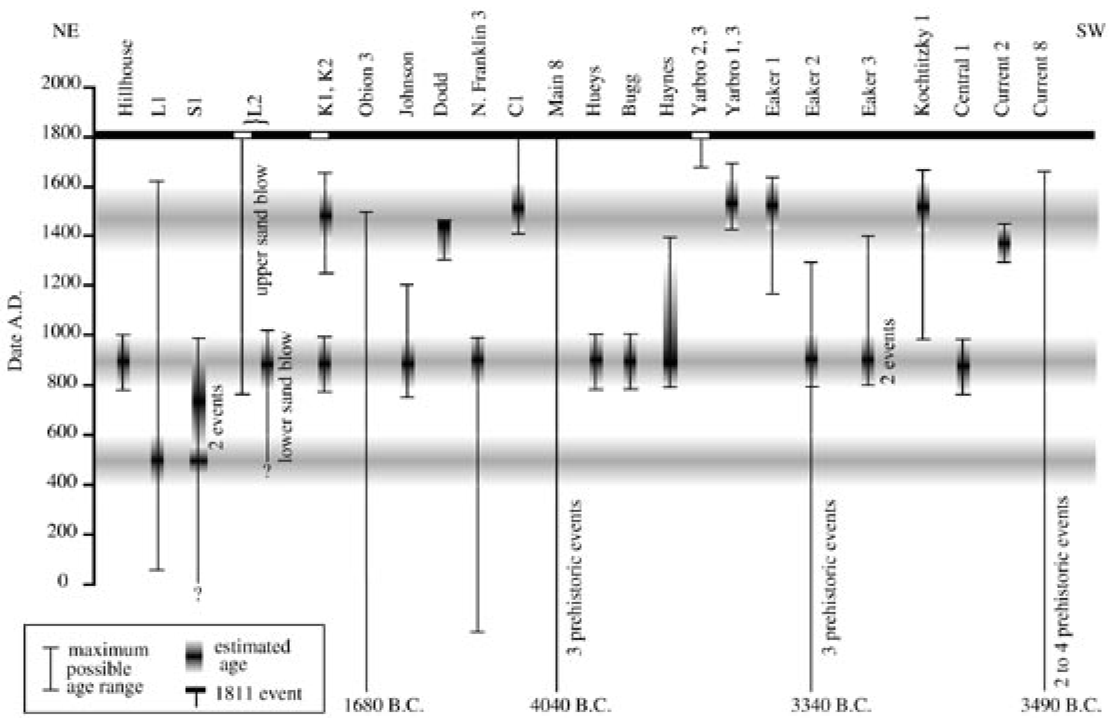

Figure 8. Earthquake chronology for the New Madrid region. Sites Current 2 and 8 are

located in Western Lowlands. Sites of other paleoseismological studies: S1, Saucier (1991); Craven (1995); L1 and L2, Li et al. (1998); K1 and K2, Kelson et al. (1996).

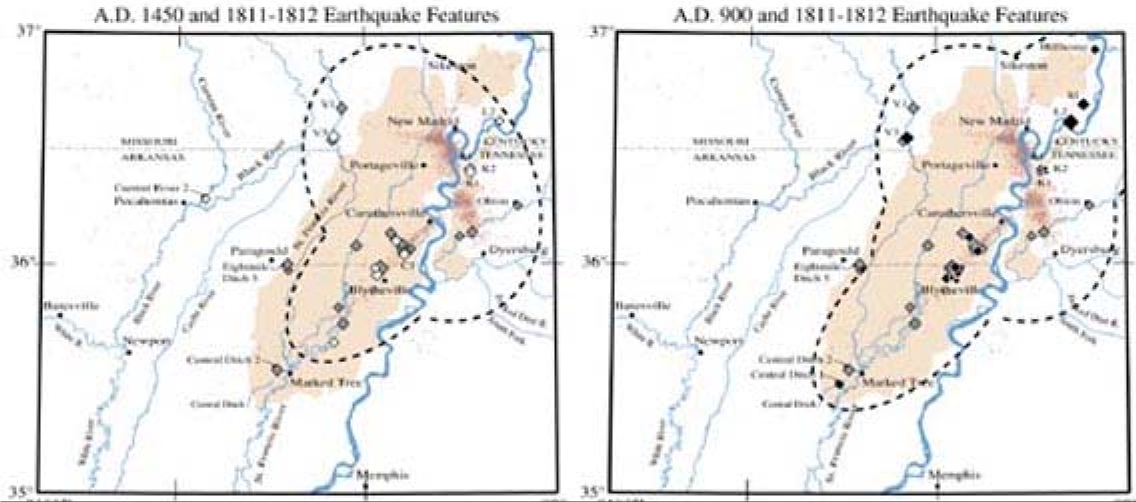

Figure 9. Distributions of sand blows and other earthquake-related features attributed to A.D. 1450 and A.D. 900 events. Locations and sizes of features related to 1811-1812 earthquake sequence shown for comparison. Possible liquefaction fields for A.D. 1450 and A.D. 900 events defined by dashed lines.

Example of Liquefaction Features Documented During Site Investigation

The Hillhouse archeological site is located east-northeast of Sikeston, Missouri, near the northeastern branch of the NMSZ (Fig. 2). This Late Woodland Native American village site was discovered and investigated by Mid-Continental Research Associates as part of an archeological survey of the New Madrid Floodway. During the archeological investigation of the site, the plow zone was removed from approximately 2000 square meters, exposing foundations of two buildings and a sweat lodge, many post-mold casts, earth ovens, and four sand dikes. The structural and stratigraphic relations of the sand dikes and cultural features provide an excellent opportunity for dating paleoliquefaction events. Two of the dikes are described in detail below.

The largest dike is 1.03 m wide, has a strike and dip of N85°W, 82°NE, and intrudes a deposit of interbedded silty clay and silty, very fine sand (Fig. 10). The dike is composed of fine sand and silty, very fine sand containing many pieces of lignite and large clasts of host deposit and black, silty clay containing artifacts. These latter clasts are similar to, and probably derived from, the overlying A horizon that was occupied by Native Americans. Radiocarbon dating of a soil sample (B-102501) collected from a pedogenic B horizon developed in the host deposit yielded a 2-sigma calibrated date with two ranges of 3780 to 3620 B.C. and 3580 to 3530 B.C. The host deposit was displaced downward by about 35 cm on the northeast side of the dike. No evidence of soil development was noted within the largest dike that occurs about 1.25 m below the scraped surface (plow zone removed). A second dike, only 12 cm wide, occurs within 1 m of the large dike and has a similar strike and dip. The smaller dike is filled with fine sand containing clasts of the overlying A horizon and extends higher in the section than the larger dike to 25 cm below the scraped surface. A very dark grayish brown, sandy soil containing illuvial fines has formed in the upper part of the smaller dike and the contact between the dike and overlying A horizon is bioturbated. Below forty centimeters from the top of the smaller dike, fines have accumulated only along the dike margins.

An 8- to 10-cm thick layer of clayey silt (interpreted as a slack-water deposit and labeled as such on Fig. 10) immediately overlies the top of the largest sand dike. This silt layer is overlain by an 80 cm-thick chaotic mixture (interpreted as fissure fill) of sand, charcoal, burned clay, and clasts of soil and host deposit. A piece of charcoal (B-102499) collected from the chaotic deposit yielded a calibrated date of A.D. 790 to 1010. A 20-cm-thick and 150-cm-wide layer of fine sand (interpreted as a reworked sand blow), containing clasts of silt and pieces of lignite, occurs above and adjacent to the top of the chaotic deposit. A very dark grayish brown, sandy soil has formed in the sand layer. The sand layer and chaotic deposit are overlain by a silty clay A horizon containing abundant ceramic and lithic artifacts. The ceramics artifacts include grog-tempered Baytown plain and Mulberry Creek cordmarked pottery, both characteristic of the Late Woodland period between A.D. 400 to 1000 (Table 1; Morse and Morse, 1983). Native American house foundations, post mold casts, and earth ovens occur nearby in this same A horizon. Charcoal (B-102500) collected from the A horizon above the small dike and level with the top of the sand layer (reworked sand blow) yielded a calibrated date of A.D. 780 to 1000. Two pieces of charcoal from the same A horizon but directly above the chaotic deposit (fissure fill) gave similar calibrated dates of A.D. 710 to 1040, and A.D. 960 to 1070 and 1080 to 1160. Potsherds recovered from soil clasts within the largest dike were also grog-tempered Baytown plain and Mulberry Creek cordmarked (R. Lafferty, pers. comm., 1998).

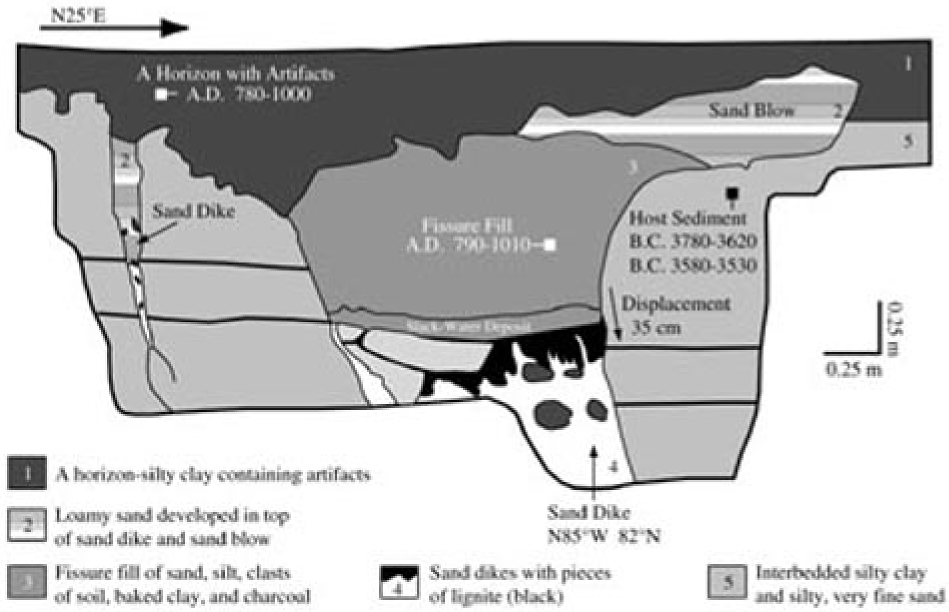

Figure 10. Trench log of sand dikes, fissure fill, and reworked sand blow at Hillhouse site.
Sand dikes are overlain by A horizon containing Late Woodland artifacts. Also, clasts of A
horizon occur in large sand dike near base of trench. Liquefaction features formed about A.D. 900 +/- 100 yr.

Table 1. Cultural periods, time spans, and associated diagnostic artifacts and plant remains
(modified from Tuttle et al., 1996).

Cultural Periods	Years (A.D./ B.C.)	Diagnostic Artifacts and Plant Remains
Historic	A.D. 1673-present	Iron, glass, glazed pottery, plastic
Late Mississippian	A.D. 1400-1673	Shell-tempered pottery - Parkin Punctate, Campbell Applique, Matthews Incised, Bell Plain, and Memphis rim mode; Nodena points
Middle Mississippian	A.D.1000-1400	Shell-tempered pottery - Parkin Punctate and Old Town Red (shell tempered, exterior slipped); Madison points; maize becomes important by

		A.D.1000-1050
Early Mississippian	A.D. 800-1000	Pottery transition - shell-tempered pottery, Varney Red Filmed pottery (shell tempered, interior slipped) and mixed temper wares
Late Woodland	A.D. 400-10002	Cordmarked and plain, sand- (Barnes) and grog- (Baytown, Mulberry Creek) tempered pottery; Table Rock Stemmed points
Middle Woodland	200 B.C.-A.D. 400	Sand- and grog-tempered pottery; dentate, stamped, and fabric-marked pottery
Early Woodland	500-200 B.C.	Punctated pottery; baked clay objects
Late Archaic	3000-500 B.C.	Stemmed projectile points; baked clay objects

1 Dougan, 1995
2 Morse and Morse (1983, 1996) use A.D. 400-700. Radiocarbon dating conducted at paleoliquefaction sites indicates that Late Woodland period extends to A.D. 1000.

The depth of the top of the largest sand dike and the nature of the materials overlying the dike suggest that an open fissure existed above the dike following its formation. Clasts of host deposit and silty clay A horizon within the large sand dike indicate that collapse of surficial material occurred at the time of dike emplacement. The clayey silt layer, immediately above the dike, is interpreted as a slack-water deposit (Fig. 10). Typically, a large volume of water is vented to the ground surface during liquefaction events. At this site, it is likely that muddy water would have been standing in depressions, including open fissures, following the event. Silt and clay suspended in water would settle to the bottom of these depressions over a period of minutes to hours. The chaotic deposit above the silt layer is interpreted as fissure fill. Clasts of occupation horizon, host sediment, and burned clay may have washed or fallen into the fissure soon after it formed. Alternatively, the natives may have used these materials to fill the open fissure. The sand layer above and adjacent to the fissure fill is interpreted as a small sand blow. Sand found in the fissure fill could have been derived from this sand blow following the event. The southwestern edge of the sand blow is reworked.

Radiocarbon dating indicates that sediment, on which the Late Woodland village developed and in which the liquefaction features formed, was deposited prior to 3000 B.C. Late Woodland ceramic artifacts in clasts of the A horizon within the largest dike and in the A horizon overlying the dikes indicate that liquefaction features at this site formed between about A.D. 700 and 1000. Radiocarbon dating of charcoal in the fissure fill provides a close maximum age of the large sand and related sand blow and indicates that they formed after A.D. 790. Radiocarbon dating of charcoal in the overlying A horizon provides a close minimum age of the liquefaction features and indicates that they formed before A.D. 1000. The combination of radiocarbon dating and artifact analysis provides a well-constrained age estimate of A.D. 900 $\pm$ 100 yr for the liquefaction features, and thus for the earthquake that induced liquefaction at this site.

Timing of New Madrid Paleoearthquakes

As demonstrated in the example above, site investigations have resulted in well-constrained age estimates for a number of liquefaction features across the region (Fig. 8). Sand blows at Dodd and Yarbro 1 and 3 are estimated to have formed between A.D. 1300 and 1670. Craven (1995) attributed a large sand blow to an earthquake during this same time period. The historic record does not indicate a New Madrid event during the period between A.D. 1600 and 1670 (Johnston, pers. comm., 1999). Therefore, the timing of the paleoearthquake can be further limited to the period prior to A.D. 1600. The age estimate (A.D. 1380 $\pm$ 70 yr) of a large sand blow at Current River 2 located in the Western Lowlands is even more limited to the earlier portion of the period. If it formed as a result of a New Madrid earthquake, the Current River sand blow might indicate that the event occurred between A.D. 1310 and 1450. Alternatively, the Current River sand blow may be related to a local earthquake source that was active at about the same time as the NMSZ. Sand blows at Bugg, Central Ditch 1, and Hueys, as well as the sand blow and dikes at Hillhouse, appear to have formed between A.D. 800 and 1000. Liquefaction features, whose ages are well-constrained, indicate that two significant earthquakes occurred in the region in A.D. 1450 $\pm$ 150 years and A.D. 900 $\pm$ 100 years.

Other liquefaction features have estimated age ranges of four hundred years or more but overlap the event times of A.D. 1450 $\pm$ 150 years and A.D. 900 $\pm$ 100 years (e.g., Haynes and Johnson sites). In some of these cases, age estimates can be further constrained by the stratigraphic position of organic samples and artifacts used to date features. Due to their large size, other liquefaction features with broader age ranges are thought to have formed during the events inferred from those features with well-constrained age estimates. For example, liquefaction features at Eaker 1 and 3 have allowable age ranges that extend into the period between A.D. 1000 and 1300. These liquefaction features are very large and likely formed as a result of very large earthquakes. There is no compelling evidence, such as a broad distribution of large sand blows, for a very large earthquake between A.D. 1000 and 1300. The occurrence of moderate to large events can not be ruled out during this period; however, liquefaction features resulting from such an event would probably be smaller than those observed. Therefore, it is more likely that the features at Eaker 1 and 3 formed during either the A.D. 900 or A.D. 1450 event.

Findings indicate that major earthquakes occurred in the New Madrid region in A.D. 1450 $\pm$ 150 years and A.D. 900 $\pm$ 100 years. This result is consistent with other paleoliquefaction studies in the region and with a study of fault-related deformation along the Reelfoot scarp (Kelson et al., 1996). In addition, there is evidence for earlier earthquakes in the region, but the age estimates of these events and the areas they affected are poorly constrained at this time.

Source Areas of New Madrid Paleoearthquakes

The source areas of paleoearthquakes that induced liquefaction in the New Madrid region can be inferred from the size and spatial distributions of paleoliquefaction features. Sand blows thought to have formed about A.D. 1450 ± 150 years (e.g., Dodd, Eaker 1, and Yarbro 1 and 3) occur along the southwestern branch of the NMSZ (Fig. 9). Other paleoliquefaction features found along several rivers and ditches across the region may have formed during this event. Vaughn (1994) documented a moderate-size sand blow of this age in the Western Lowlands along the St. Francis River. Kelson et al. (1996) attributed an episode of graben formation along the Reelfoot scarp to an event between A.D. 1260 and 1650. Sand blows that formed circa A.D. 1450 range in thickness from 0.3 to 1 m.

Sand blows thought to have formed about A.D. 900 ± 100 years (e.g., Bugg, Central Ditch 1, Eaker 2 and 3, Hillhouse, Hueys, and possibly Haynes, Johnson 5, and New Franklin 3) are broadly distributed from southwest of Marked Tree, Arkansas, to northeast of Sikeston, Missouri (Fig. 9). Other paleoliquefaction features found along several rivers and ditches also may have formed during this event. Li et al. (1998) found a large sand blow east of New Madrid, Missouri, that probably formed about A.D. 900. Not far to the north, Saucier (1991) found a moderate-size sand blow at the Towosahgy archeological site that could have formed during the same earthquake. Vaughn (1994) documented a large sand blow of this age in the Western Lowlands along the St. Francis River. Kelson et al. (1996) attributed an episode of liquefaction and graben formation along the Reelfoot scarp to an event between A.D. 780 and 1000. Sand blows that formed circa A.D. 900 range in thickness from 0.2 to 1.7 m.

The New Madrid earthquake sequence of 1811-1812 can serve as a regional calibration event for paleoearthquakes. Sand blows thought to have formed during the 1811-1812 earthquakes (e.g., Brooke and Yarbro 2 and 3 sites) are broadly distributed from Marked Tree, Arkansas, in the south, to Paragould, Arkansas, in the west, and to Obion, Tennessee, in the east (Fig. 9). In addition, Vaughn (1994) documented historic sand blows in the Western Lowlands along the St. Francis River, and Kelson et al. (1996) attributed sand dikes along the Reelfoot scarp to the 1811-1812 earthquakes. Li et al. (1998) found a small sand blow east of New Madrid, Missouri, that probably formed during the 1811-1812 earthquakes. Most sand blows that formed in 1811-1812 range in thickness from 0.5 to 1 m. Additional work is needed to determine the size distribution of historic sand blows in the northern part of the NMSZ.

The size and spatial distributions of sand blows that formed during the A.D. 1450 event is similar to, but slightly less extensive than, that of historic sand blows (Fig. 9). The size and spatial distribution of sand blows that formed during the A.D. 900 event is also similar to that for historic sand blows. Apparent differences in these distributions occur in the vicinity of the Obion River, Eightmile Ditch, and the New Madrid Floodway. It should be remembered that only a small sample of sand blows, especially for the 1811-1812 and A.D. 1450 events, has been studied so far. As additional reconnaissance and detailed investigations are carried out, a more complete picture of the distribution of liquefaction features of various ages will emerge. Nevertheless, the similarities in the size and spatial distributions of historic and paleoliquefaction features are striking. Furthermore, there is a close spatial correlation of both historic and paleoliquefaction features with the NMSZ, indicating that the NMSZ almost certainly was the source of the two paleoearthquakes, as it was for the 1811-1812 earthquake sequence.

Magnitudes of New Madrid Paleoearthquakes

Two approaches to estimating magnitudes of paleoearthquakes from liquefaction features have been applied in the New Madrid region. One approaches involves the use of Ambraseys' (1988) relation between moment magnitude and epicentral distance to surface manifestation of liquefaction in combination with the comparison of the size and spatial distributions of paleoliquefaction features with historic liquefaction features (Tuttle, 1999). The other approach involves *in situ* testing of geotechnical properties and assessment of liquefaction potential.

As discussed above, the NMSZ is the likely source of the A.D. 1450 and A.D. 900 earthquakes. Although the full extent of liquefaction has not been determined, minimum magnitudes for the A.D. 1450 and A.D. 900 events can be estimated from the currently known spatial distributions of liquefaction features attributed to these events. Taking the mid-points of the liquefaction fields as the epicenters of the earthquakes, epicentral distances to the farthest liquefaction sites are 70 km for the A.D. 1450 event and 100 km for the A.D. 900 event. Using Ambraseys' relation (1988), the A.D. 1450 and A.D. 900 events are estimated to be at least of **M** 6.7 and **M** 6.9, respectively (Fig. 11). As additional liquefaction features are found and dated, liquefaction fields and thus epicentral distances to farthest liquefaction features are likely to increase, leading to greater magnitudes estimates. As described above, the size and spatial distributions of sand blows in the New Madrid region are quite similar for the 1811-1812, A.D. 1450, and A.D. 900 events. This suggests that the paleoearthquake sequences are comparable in location and magnitude to the 1811-1812 event. Given that Ambraseysí relation suggests that the largest of the 1811-1812 earthquakes was of **M** $\geq$ 7.6, the A.D. 1450 and A.D. 900 events arelikely to have included at least one earthquake in this magnitude range.

Geotechnical testing and analysis of liquefaction potential was recently carried out for a few liquefaction sites where the ages of sand blows are well constrained, including Brooke, Dodd, and Johnson sites near Steele, Missouri, and Bugg, Hueys, and Sigman sites near Blytheville, Arkansas. Schneider et al. (1999) found that sediments at the sites are not especially susceptible to liquefaction and estimated that it would take an earthquake of **M** 7.5 to 8.3 to induced liquefaction at all of the sites. This result is similar to the magnitude estimate of **M** $\geq$ 7.6 from Ambraseys' ralation for the largest of the 1811-1812 earthquakes. Although these initial results are promising, much work remains to characterize liquefaction susceptibility at distal liquefaction sites and at non-liquefaction sites within the meizoseismal area and to account for affects of age and recurrent liquefaction on the liquefied layer when back-calculating earthquake magnitudes from modern field measurements.

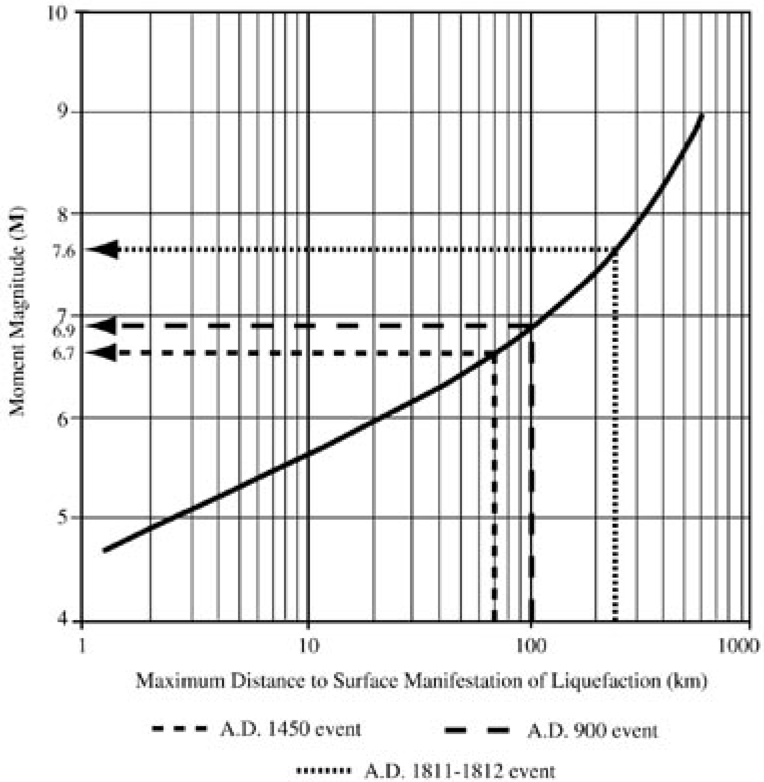

Figure 11. Relation between earthquake magnitude and distance to liquefaction developed
from worldwide database of shallow earthquakes (Ambraseys, 1988). Distance to farthest
known liquefaction features indicate that A.D. 1450 and A.D. 900 events were at least of **M** 6.7 and 6.9, respectively. Similarity in size distribution of historic and prehistoric sand
blows, however, suggest that paleoearthquakes were comparable in size to 1811-1812 events or at least of **M** 7.6.

Conclusion or Lessons Learned in the New Madrid Seismic Zone

To estimate timing, source areas, and magnitudes of paleoearthquakes from liquefaction features, it is necessary to document many liquefaction features across a region and to constrain the ages of those features as closely as possible. This goal is best achieved by conducting both regional reconnaissance and detailed site investigations. It is important to evaluate many sites across a region to identify the best sites for dating paleoliquefaction features and to define the size and spatial distributions of liquefaction features produced by each event.

Detailed investigations often yield information needed to constrain the age estimates of liquefaction features. In the NMSZ, for example, detailed investigations have made it possible to recognize two different events during an eight-hundred-year period and to tightly constrain (± 100 to 150 years) the age estimates of liquefaction features. Given the current methodology of dating organic material in horizons that bound sand blows and the uncertainty in age estimates that results, it would be desirable to develop high precision methods for dating liquefaction features directly. In the meantime, care must be taken to collect samples that will provide close minimum and maximum dates for individual liquefaction features and to express uncertainty (two-sigma) in age estimates related to dating practices. Well-constrained ages of individual liquefaction features should provide the basis for estimating the timing of paleoearthquakes and correlating features across a region. The size and spatial distributions of similar-age features are used to estimate source areas and magnitudes of paleoearthquakes. Therefore, if ages of liquefaction features are not well-constrained, it is difficult to estimate timing, source areas, and magnitudes of earthquakes with much certainty.

Modern or historic earthquakes that induced liquefaction in the same region can serve as calibration events for paleoearthquakes. In the NMSZ, for example, comparison of the size and spatial distributions of historic and pre-1811 sand blows suggests source areas and magnitudes for paleoearthquakes similar to the very large to great earthquakes of 1811-1812. Much can be learned about interpreting paleoliquefaction features from studying liquefaction features that formed during modern earthquakes. Additional studies in various tectonic settings of the size and spatial distributions of liquefaction features, coupled with geotechnical testing at the liquefaction sites, could further advance the use of liquefaction features in paleoseismology.

Acknowledgments

Buddy Schweig, John Sims, and Ann Wylie reviewed an early version of this manuscript and provided many helpful comments and suggestions. Buddy Schweig also participated in many of the site investigations of liquefaction features in the NMSZ. Bob Lafferty conducted archeological investigations at several of the liquefaction sites and Neal Lopinot performed archeobotanical analysis of plant remains. Noel Barstow, Jonathan Collier, Kathleen Dyer-Williams, Marion Haynes, Pedro Alfaro Garcia, Luis Pena, and Janine Savage participated in various aspects of the paleoliquefaction study in the New Madrid region. Tom Holzer and John Tinsley provided thoughtful reviews of this manuscript for which I am grateful. Research presented in this manuscript was supported by grants from the US Geological Survey (143493G-2352, 143495G-2633, and 1434HQ97GR-03082) and the US Nuclear Regulatory Commission (0495073 and 0497065). The views and conclusions presented in this paper are those of the author and should not be interpreted as necessarily representing the official policies, either expressed or implied, of the US Government.

References Cited

Allen, J.R.L., 1982, Sedimentary structures: their character and physical basis, Elsevier, Amsterdam.

Ambraseys, N.N., 1988, Engineering Seismology: earthquake engineering and structural dynamics, Journal of the International Association of Earthquake Engineering, v. 17, p. 1-105.

Amick, D., Gelinas, R., Maurath, G., Cannon, R., Moore, D., Billington, E., and Kemppinen, H., 1990, Paleoliquefaction features along the Atlantic Seaboard, US Nuclear Regulatory Commission, NUREG/CR-5613, 146 p.

Arias, A., 1970, A measure of earthquake intensity, *in* Hansen, R.J., ed., Seismic design of nuclear power plants, MIT Press, Cambridge, MA.

Audemard, F., and de Santis, F., 1991, Survey of liquefaction structures induced by recent moderate earthquakes, Bulletin of the International Association of Engineering Geology, v. 44, p. 5-16.

Braile, L., Hinze, W., Sexton, J., Keller, R., and Lidiak, E., 1984, Tectonic development of the New Madrid seismic zone, *in* Gori, P.L., and Hayes, W.W., eds., Proceedings, Symposium on the New Madrid earthquakes, US Geological Survey Open-File Report 84-770, p. 204-233.

Braile, L.W., Hinze, W.J., Von Frese, R.R.B., and Keller, G.R., 1988, Seismic properties of the crust and upper-most mantle of North America, *in* Pakiser, L.C., and Mooney, W., eds., Geophysical Framework of the Continental United States, Geological Survey Memoir, 172.

Buschbach, T.C., and Schwalb, H.R., 1984, Sedimentary geology of the New Madrid seismic zone, *in* Gori, P.L., and Hayes, W.W., eds., Proceedings, Symposium on the New Madrid earthquakes, US Geological Survey Open-File Report 84-770, p. 64-96.

Craven, J.A., III, 1995, Paleoseismological study in the New Madrid seismic zone using geological and archeological features to constrain ages of liquefaction deposits, M.S. Thesis, Memphis, Tennessee, University of Memphis, 51 p.

Dougan, M., 1995, An Arkansas odyssey, Little Rock, Rose Publishing, 684 p.

Fuller, M.L., 1912, The New Madrid earthquake, US Geological Survey Bulletin 494, 119 p.

Holzer, T.L., and Clark, M.M., 1993, Sand boils without earthquakes, Geology, v. 21, p. 873-876.

Ishihara, K., 1985, Stability of natural soils during earthquakes, Proceedings of the Eleventh International Conference on Soil Mechanics and Foundation Engineering, San Francisco, v. 1, p. 321-376.

Johnston, A.C., 1996, Seismic moment assessment of stable continental earthquakes, Part III: 1811-1812 New Madrid, 1886 Charleston and 1755 Lisbon, Geophysical Journal International, v. 126, p. 314-344.

Johnston, A.C., and Schweig, E.S., 1996, The enigma of the New Madrid earthquakes of 1811-1812, Annual Review of Earth and Planetary Sciences, v. 24, p. 339-384.

Kayen, R.E., and Mitchell, J.K., 1997, Assessment of liquefaction potential during earthquakes by Arias intensity, Journal of Geotechnical and Geoenvironmental Engineering, v. 123, n. 12, p. 1162-1174.

Kelson, K.I., Simpson, G.D., Van Arsdale, R.B., Harris, J.B., Haradan, C.C., and Lettis, W.R., 1996, Multiple Holocene earthquakes along the Reelfoot fault, central New Madrid seismic zone, Journal of Geophysical Research, v. 101, n. B3, p. 6151-6170.

Kuribayashi, E., and Tatsuoka, F., 1975, Brief review of liquefaction during earthquakes in Japan, Soils and Foundations, v. 15, p. 81-92.

Li, Y., Craven, J., Schweig, E.S., Obermeier, S.F., 1996, Sand boils induced by the 1993 Mississippi River flood: Could they one day be misinterpreted as earthquake-induced liquefaction?, Geology, v. 24, n. 2, p. 171-174.

Li, Y., Schweig, E., Tuttle, M.P., and Ellis, M.A., 1998, Evidence for large prehistoric earthquakes in the northern New Madrid seismic zone, central United States, Seismological Research Letters, v. 69, p. 270-276.

Lowe, D.R., 1975, Water escape structures in coarse-grained sediment, Sedimentology, v. 22, p. 157-204.

Morse, D.F., and Morse, P.A., 1983, Archaeology of the central Mississippi Valley, Academic Press, San Diego, 345 p.

Morse, D.F., and Morse, P.A., 1996, Northeast Arkansas, *in* McNutt, C. H., ed., Prehistory of the Central Mississippi Valley, University of Alabama Press, Tuscaloosa, p. 113-136.

Munson, P.J., Obermeier, S.F., Munson, C.A., and Hajic, E.R., 1997, Liquefaction evidence for Holocene and Latest Pleistocene seismicity in the southern halves of Indiana and Illinois: A preliminary overview, Seismological Research Letters, v. 68, n. 4, p. 521-536.

Murray, G.E., 1961, Geology of the Atlantic and Gulf coastal province of North America, Harper and Brothers, New York, 692 p.

Obermeier, S.F., Gohn, G.S., Weems, R.E., Gelinas, R.L., and Rubin, M., 1985, Geologic evidence for recurrent moderate to large earthquakes near Charleston, South Carolina, Science, v. 227, p. 408-411.

Obermeier, S.F., 1989, The New Madrid Earthquakes: An engineering-geologic interpretation of relict liquefaction features, US Geological Survey, Professional Paper 1336-B, 114 p.

Obermeier, S.F., Jacobson, R.B., Smoot, J.P., Weems, R.E., Gohn, G.S., Monroe, J.E., and Powars, D.S., 1990, Earthquake-induced liquefaction features in the coastal setting of South Carolina and in the fluvial setting of the New Madrid seismic zone, U.S. Geological Survey, Professional Paper 1504, 44 p.

Obermeier, S.F., Martin, J.R., Frankel, A.D., Youd, T.L., Munson, P.J., Munson, C.A., and Pond, E.C., 1993, Liquefaction evidence for one or more strong Holocene earthquakes in the Wabash Valley of southern Indiana and Illinois, with a preliminary estimate of magnitude, U.S. Geological Survey, Professional Paper 1536, 27 p.

Obermeier, S.F., 1996, Using liquefaction-induced features for paleoseismic analysis, *in* McCalpin, J.P., ed., Paleoseismology, Academic Press, San Diego, CA, p. 331-396.

Owen, H.G., 1987, Deformation processes in unconsolidated sands, Geological Society of London Special Publication, v. 29, p. 11-24.

Pond, E.C., 1996, Seismic parameters from the central United States based on paleoliquefaction evidence in the Wabash Valley, PhD. Dissertation, Virginia Poytechnic Institute, Blacksburg, Virginia, 583 p.

Russ, D.P., 1982, Style and significance of surface deformation in the vicinity of New Madrid, Missouri *in* McKeown, F.A. and Pakiser, L.C., eds., Investigations of the New Madrid, Missouri, earthquake region, U.S. Geological Survey Professional Paper 1236, p. 94-114.

Saucier, R.T., 1977, Effects of the New Madrid earthquake series in the Mississippi alluvial valley, U.S. Army Corps of Engineers Waterways Experiment Station, Miscellaneous Paper S-77-5.

Saucier, R.T., 1991, Geoarchaeological evidence of strong prehistoric earthquakes in the New Madrid (Missouri) seismic zone, Geology, v. 19, p. 296-298.

Saucier, R.T., 1994, Geomorphology and Quaternary geologic history of the lower Mississippi, U.S. Army Corps of Engineers Waterways Experiment Station, v. I and II, 364 p. and 28 plates.

Schneider, J., Camp, B., and Mayne, P.W., 1999, Soil liquefaction assessment in mid-America by seismic piezocone tests, Seismological Society of America, Eastern Section Meeting, Program and Abstracts, p. 19-20.

Seed, H.B., 1979, Soil liquefaction and cyclic mobility evaluation for level ground during earthquakes, Proceedings of the American Society of Civil Engineering, Journal of Geotechnical Engineering, v. 105, p. 201-255.

Seed, H.B., and Idriss, I.M., 1982, Ground motions and soil liquefaction during earthquakes, Earthquake Engineering Research Institute, University of California, Berkeley, 134 p.

Seed, H.B., Idriss, I.M., and Arango, I., 1983, Evaluation of liquefaction potential using field performance data, Journal of Geotechnical Engineering, v. 109, p. 458-482.

Seed, H.B., Tokimatsu, K., Harder, L.F., and Chung, R.M., 1985, Influence of SPT procedures in soil liquefaction resistance evaluation, Journal of Geotechnical Engineering, v. 111, p. 1425-1445.

Sims, J.D., 1973, Earthquake-induced structures in sediments of Van Norman Lake, San Fernando California, Science, v. 182, p. 161-163.

Sims, J.D., and Garvin, C.D., 1995, Recurrent liquefaction at Soda Lake, California, induced by the 1989 Loma Prieta earthquake, and 1990 and 1991 aftershocks: Implications for paleoseismicity studies, Seismological Society of America Bulletin, v. 85, p. 51-65.

Street, R., and Nuttli, O., 1984, The central Mississippi Valley earthquakes of 1811-1812, *in* Proceedings of the Symposium on "The New Madrid Seismic Zone," U.S. Geological Survey Open-File Report 84-770, p. 33-63.

Stuiver, M., Long A., Kra, R. S., and Devine, J. M., 1993, Calibration - 1993, Radiocarbon, v. 35, n. 1, 244 p.

Talwani, P., and Cox, J., 1985, Paleoseismic evidence for recurrence of earthquakes near Charleston, South Carolina, Science, v. 228, p. 379-381.

Tuttle, M.P., Law, T., Seeber, L., and Jacob, K., 1990, Liquefaction and ground failure induced by the 1988 Saguenay, Quebec earthquake, Canadian Geotechnical Journal, v. 27, p. 580-589.

Tuttle, M.P., and Seeber, L., 1991, Historic and prehistoric earthquake-induced liquefaction in Newbury, Massachusetts, Geology, v. 19, p. 594-597.

Tuttle, M.P., Cowie, P., and Wolf, L., 1992, Liquefaction induced by modern earthquakes as a key to paleoseismicity: A case study of the 1988 Saguenay event, Proceedings of the

Nineteenth International Water Reactor Safety Information Meeting, NUREG/CP-0119, v. 3, p. 437-462.

Tuttle, M., and Barstow, N., 1996, Liquefaction-related ground failure: A case study in the New Madrid seismic zone, central United States, Bulletin of the Seismological Society of America, v. 86, n. 3, p. 636-645.

Tuttle, M.P., Lafferty, R.H., Guccione, M.J., Schweig, E.S., Lopinot, N., Cande, R.F., Dyer-Williams, K., Haynes, M., 1996, Use of archaeology to date liquefaction features and seismic events in the New Madrid seismic zone, central United States, Geoarchaeology, v. 11, n. 6, p. 451-480.

Tuttle, M.P., Collier, J., Wolf, L.W., and Lafferty, R.H., 1999, New evidence for a large earthquake in the New Madrid seismic zone between A.D. 1400 and 1670, Geology, v. 27, n. 9, p. 771-774.

Tuttle, M.P., 1999, Late Holocene earthquakes and their implications for earthquake potential of the New Madrid seismic zone, central United States, Ph.D. Dissertation, University of Maryland, 250 p.

Vaughn, J.D., 1994, Paleoseismological studies in the Western Lowlands of southeastern Missouri, Final Report to the U.S. Geological Survey for grant number 14-08-0001-G1931, 27 p.

Wesnousky, S.G., and Leffler, L., 1992, The repeat time of the 1811 and 1812 New Madrid earthquakes: A geological perspective, Bulletin of Seismological Society of America, v. 84, n. 4, p. 1756-1785.

Wesnousky, S.G., and Johnson, D.L., 1996, Stratigraphic, paleosol and C-14 evidence for a large pre-1811 magnitude earthquake in the New Madrid seismic zone, Seismological Research Letters, v. 67, n. 2, p. 60.

Wilson, R.C., 1993, Relation of Arias intensity to magnitude and distance in California, U.S. Geological Survey, Open-File Report 93-556.

Youd, T.L., 1973, Liquefaction, flow and associated ground failure, U.S. Geological Survey, Circular 688, 12 p.

Youd, T.L., 1984, Geologic effects ? Liquefaction and associated ground failure, U.S. Geological Survey, Open-File Report 84-760, p. 210-232.

Youd, T.L., and Perkins, D.M., 1987, Mapping of liquefaction severity index, Journal of Geotechnical Engineering, v. 113, n. 11, p. 1374-1392.

Youd, T.L., and Garris, C.T., 1995, Liquefaction-induced ground-failure disruption, Journal of Geotechnical Engineering, v. 121, n. 11, p. 805-809.

Zoback, M.L., and Zoback, M.D., 1989, Tectonic stress field of the continental United States, *in* Pakiser, L.C., and Mooney, W.D., eds., Geophysical framework of the continental United States, Geological Society of America Memoir 172, p. 523-539.